

## Original Article

## Multimodal navigated skull base tumor resection using image-based vascular and cranial nerve segmentation: A prospective pilot study

Parviz Dolati, Abdulkarim Gokoglu, Daniel Eichberg, Amir Zamani, Alexandra Golby, Ossama Al-Mefty

Department of Neurosurgery, Harvard Medical School, Brigham and Women's Hospital, Boston, Massachusetts, USA

E-mail: \*Parviz Dolati - [neuro81ward@yahoo.com](mailto:neuro81ward@yahoo.com); Abdulkarim Gokoglu - [akerimg@hotmail.com](mailto:akerimg@hotmail.com); Daniel Eichberg - [deichberg35@gmail.com](mailto:deichberg35@gmail.com); Amir Zamani - [azamani@partners.org](mailto:azamani@partners.org); Alexandra Golby - [agolby@partners.org](mailto:agolby@partners.org); Ossama Al-Mefty - [oalmefty@partners.org](mailto:oalmefty@partners.org)  
\*Corresponding author

Received: 13 May 15 Accepted: 31 August 15 Published: 19 November 15

### Abstract

**Background:** Skull base tumors frequently encase or invade adjacent normal neurovascular structures. For this reason, optimal tumor resection with incomplete knowledge of patient anatomy remains a challenge.

**Methods:** To determine the accuracy and utility of image-based preoperative segmentation in skull base tumor resections, we performed a prospective study. Ten patients with skull base tumors underwent preoperative 3T magnetic resonance imaging, which included thin section three-dimensional (3D) space T2, 3D time of flight, and magnetization-prepared rapid acquisition gradient echo sequences. Imaging sequences were loaded in the neuronavigation system for segmentation and preoperative planning. Five different neurovascular landmarks were identified in each case and measured for accuracy using the neuronavigation system. Each segmented neurovascular element was validated by manual placement of the navigation probe, and errors of localization were measured.

**Results:** Strong correspondence between image-based segmentation and microscopic view was found at the surface of the tumor and tumor-normal brain interfaces in all cases. The accuracy of the measurements was  $0.45 \pm 0.21$  mm (mean  $\pm$  standard deviation). This information reassured the surgeon and prevented vascular injury intraoperatively. Preoperative segmentation of the related cranial nerves was possible in 80% of cases and helped the surgeon localize involved cranial nerves in all cases.

**Conclusion:** Image-based preoperative vascular and neural element segmentation with 3D reconstruction is highly informative preoperatively and could increase the vigilance of neurosurgeons for preventing neurovascular injury during skull base surgeries. Additionally, the accuracy found in this study is superior to previously reported measurements. This novel preliminary study is encouraging for future validation with larger numbers of patients.

**Key Words:** Blood vessels, cranial nerves, image segmentation, magnetic resonance imaging, neuronavigation, skull base neoplasms

#### Access this article online

**Website:**

[www.surgicalneurologyint.com](http://www.surgicalneurologyint.com)

**DOI:**

10.4103/2152-7806.170023

**Quick Response Code:**

This is an open access article distributed under the terms of the Creative Commons Attribution-NonCommercial-ShareAlike 3.0 License, which allows others to remix, tweak, and build upon the work non-commercially, as long as the author is credited and the new creations are licensed under the identical terms.

**For reprints contact:** [reprints@medknow.com](mailto:reprints@medknow.com)

**How to cite this article:** Dolati P, Gokoglu A, Eichberg D, Zamani A, Golby A, Al-Mefty O. Multimodal navigated skull base tumor resection using image-based vascular and cranial nerve segmentation: A prospective pilot study. *Surg Neurol Int* 2015;6:172.

<http://surgicalneurologyint.com/Multimodal-navigated-skull-base-tumor-resection-using-image-based-vascular-and-cranial-nerve-segmentation:-A-prospective-pilot-study/>

## BACKGROUND

Tumors of the skull base region represent some of the most challenging lesions to resect. Because skull base tumors are critically and deeply located, access and total removal have always been the main challenges in the surgical management of such cases. Additionally, invasion of bone and critical neurovascular structures often impedes complete resection of skull base neoplasms. For these reasons, it is unsurprising that skull base procedures entail a risk of new permanent cranial nerve deficits and may necessitate a subtotal resection, which may lead to the regrowth of the residual tumor.<sup>[46]</sup> Thus, the fundamental aim of skull base tumor surgery is to maximize resection while minimizing damage to involved or adjacent neural and vascular structures, thereby avoiding new neurological deficits.

Interactive intraoperative image guidance is rapidly becoming an indispensable neurosurgical technique.<sup>[9,10,33,42]</sup> Preoperative planning, intraoperative identification of anatomic landmarks, and avoidance of critical structures are particularly essential tasks in complex tumor resections because skull base lesions frequently encase or extend into the neighboring normal neural and vascular elements.<sup>[24,38]</sup> Thus, image-guidance reduces surgical morbidity while increasing the surgeon's confidence of achieving full resection without impinging upon nearby critical structures.<sup>[24]</sup> Such assistance is provided by image-guided surgery, a technique that affords truly useful feedback to the surgeon in planning and simulation of the surgical approach, intraoperative orientation, avoidance of vital neurovascular structures, and assessing the completeness of resection. Image-guided surgery ensures advanced warning of proximity to important anatomical structures and identifies the full spatial extent of tumors.<sup>[20]</sup>

Although current image guidance is primarily dependent on preoperative magnetic resonance images (MRIs) and does not account for brain shift during surgery,<sup>[7]</sup> it has been demonstrated that skull base cases are significantly less affected by brain shift than intrinsic brain lesions cases.<sup>[7]</sup> For this reason, the reliance of image guidance on preoperative MRIs may not be a significant concern.

Here, we provide a prospective pilot study in which ten patients with skull base tumors underwent image-based preoperative vascular and neural element segmentation with three-dimensional (3D) reconstruction for intraoperative guidance, as well as intraoperative validation of each segmented neural or vascular element. We aimed to determine the accuracy and utility of image-based preoperative segmentation in skull base tumor resections. We hypothesized that this preoperative segmentation can improve resection rate, minimize surgical morbidities, and increase the accuracy of localization compared to previously reported accuracies.

## PROCEDURE

### Study size and setting

After approval by the Hospital Institutional Review Board, a total of 10 patients with skull base tumors underwent image-based preoperative vascular neural elements and tumor segmentation with 3D reconstruction. These procedures took place at a single institution from December 2013 to May 2014, and data were prospectively collected and retrospectively reviewed.

### Participants

Patient selection for the use of image-guided techniques was based solely on surgeon preference; there were no qualifying or disqualifying factors. The authors have no personal interest in the system used. Adult patients with skull base tumors of any type were included.

### Image acquisition

The patients underwent preoperative 3T MRI, which included thin section 3D space T2, 3D time of flight, magnetization-prepared rapid acquisition gradient echo, and dynamic computed tomography (CT) angiography. An expert neuroradiologist reviewed the images before segmentation. Subsequently, imaging sequences were loaded in either BrainLAB iPlan Net (Brainlab AG, Munich, Germany) for 8 patients, or Stryker (Stryker, Kalamazoo, Michigan, USA) for 2 patients, for fusion, segmentation, and preoperative planning. After fixing patients' heads with a Mayfield 3-point fixation system, careful patient registration to the intraoperative neuronavigation system, and surgical exposure, each segmented neural or vascular element was validated by manual placement of the navigation probe over each target in different stages of tumor resection, and screenshots were captured. Errors of localization were measured in mm.

### Study design and data sources

This pilot study was a prospective validation study. Primary endpoints were defined as correspondence between image-based segmentation and microscopic view at the surface of the tumor and tumor-brain interfaces, major arteries, veins, and venous sinuses or cranial nerves with measurements of errors in mm [Figure 1 Panels A-H]. Five different neurovascular landmarks were identified in each case and measured for the accuracy of localization using the neuronavigation system. This correspondence was determined by the surgeons at the time of surgery by measuring the distance between the tip of the neuronavigation probe and the target and rechecked by another neurosurgeon. An expert neuropathologist determined tumor pathology. Extent of resection was determined by the surgeons at the time of surgery and was confirmed by postoperative brain MRI. In meningioma resection cases, the Simpson grading system was used to evaluate the extent of resection.<sup>[32]</sup>

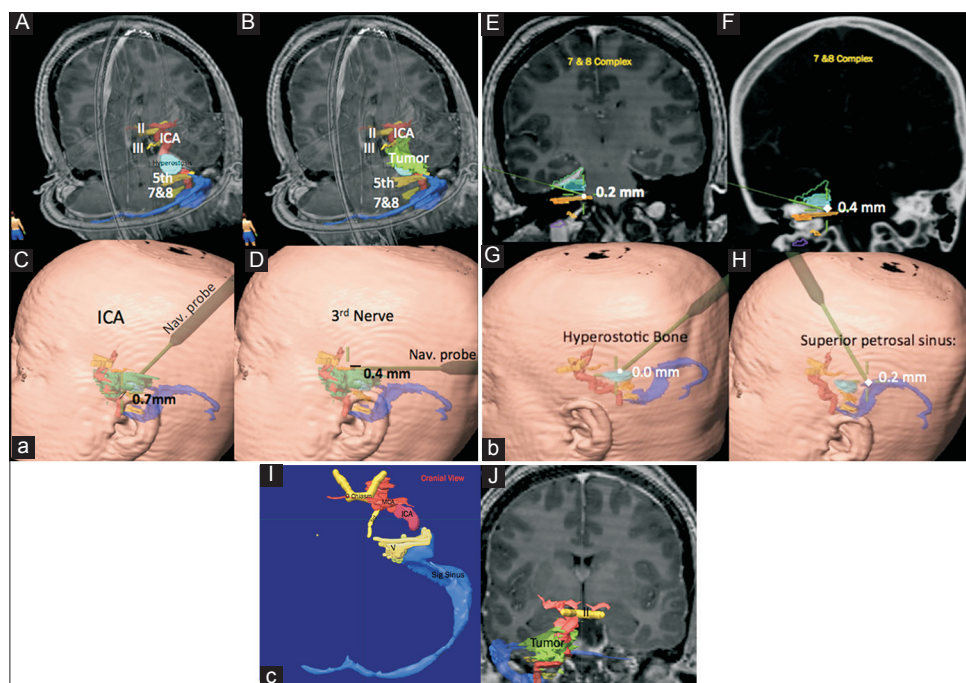


**Figure 1:** (a) Preoperative segmentation of the right petrous apex meningioma; Panel A, showing only the hyperostosis and Panel B, showing tumor at the top of the hyperostosis along with segmentation of the cranial nerves, II, III, V and VII and VIII complex. Panels C and D are intraoperative localization of the internal carotid artery and cranial nerve III, which showing also navigation errors from the targets (0.7 mm and 0.4 mm, respectively). (b) Panels E and F show cranial nerves 7 and 8 complex in magnetic resonance imaging and computed tomography scan, respectively. Panel G, shows navigation of the hyperostotic bone after resection of the soft tissue and finally Panel H shows localization of the superior petrosal sinus. The numbers on the panels are the accuracy errors from the target. (c) Panels J and I show object creation after segmentation of the involved regions; Panel I shows cranial view with tumor removed and Panel J shows frontal view with tumor in place

## Statistical methods

Patients' clinical and tumor characteristics (age, sex, tumor pathology, and, completeness of resection) were evaluated using the mean and range for continuous variables and the frequency count for categorical factors. The Sørensen–Dice index was used to compare the correspondence between image-based segmentation and microscopic view at the surface of the tumor and tumor-normal brain interfaces, as well as the major arteries, veins, and venous sinuses. The average accuracy of localization was evaluated using the mean and standard deviation (SD).

## RESULTS

### Descriptive data

#### Participants

The mean age was 57.8 years, and there were 4 male and 6 female patients [Table 1]. The most common presentation was diplopia (30%), followed by ataxia (10%), aphasia and right pronator drift (10%), abducens nerve palsy (10%), facial nerve palsy (10%), hemiparesis (10%), right visual field loss (10%), and trigeminal neuralgia and numbness (10%).

#### Tumor pathology

Five patients (50%) had meningothelial meningioma WHO Grade I, 2 patients (20%) had atypical meningioma WHO

Grade II, 1 patient (10%) had chordoma, 1 patient (10%) had left Meckel's cave Schwannoma, and 1 patient (10%) had anaplastic meningioma WHO Grade III.

### Operative data

Reasonable correspondence between image-based segmentation and the microscopic view was found at the surface of the tumor and tumor-normal brain interfaces in all cases (Dice-coefficient = 1). The accuracy of the measurements was  $0.45 \pm 0.21$  mm (mean  $\pm$  SD). This information reassured the surgeon and prevented vascular injury during different stages of tumor resection. Preoperative segmentation of the related cranial nerves was technically possible in only 80% of cases. However, image-guidance helped the surgeon localize the involved cranial nerves in all of these segmented cases reliably.

### Resection rate

Eight patients (90%) had either gross total resection or Simpson Grade II meningioma resection, and 1 patient (10%) had Simpson Grade III meningioma resection.

### Complications

The postoperative complication was noticed in only 1 patient who suffered transient partial abducens nerve palsy and Horner syndrome.

**Table 1: Demographic data, clinical presentation, pathology, location, resection rate, immediate complications, and errors of localization of 10 patients in this study**

Patients	Gender	Age	Presentation	Pathology	Location	Resection rate	Complication	Navigation system	Errors of localization (mm)
1	Male	41	Diplopia, facial pain	Chordoma	Petrous apex and clivus	Gross total	None	BrainLAB iPlan Net	0.21
2	Male	57	Diplopia, aphasia	Schwannoma	Sphenoid wing	Gross total	Abducens nerve palsy, Horner syndrome	BrainLAB iPlan Net	0.20
3	Female	70	Seizure, right hemiparesis	Anaplastic meningioma	Frontal lobe	Simpson Grade II	Facial pain	BrainLAB iPlan Net	0.28
4	Female	64	Facial nerve palsy, hearing loss	Atypical meningioma	Sphenoid wing, middle fossa	Gross total	None	Stryker	0.55
5	Male	53	Headache, ataxia	Meningothelial meningioma	Petroclival	Simpson Grade II	None	BrainLAB iPlan Net	0.43
6	Male	63	Aphasia, right pronator drift	Atypical meningioma	Midline skull base	Simpson Grade II	None	BrainLAB iPlan Net	0.74
7	Female	55	Right visual loss	Meningothelial meningioma	Right sphenoid wing	Simpson grade II	None	BrainLAB iPlan Net	0.38
8	Female	42	Right sided facial pain	Meningothelial meningioma	Tentorial	Simpson Grade II	None	BrainLAB iPlan Net	0.53
9	Female	70	Right abducens nerve palsy	Meningothelial meningioma	Clivus	Simpson Grade III	None	Stryker	0.38
10	Female	63	Headache, diplopia	Meningothelial meningioma	Cavernous sinus	Simpson Grade II	None	BrainLAB iPlan Net	0.84
Mean ± SD (mm)									0.45 ± 0.21

SD: Standard deviation

## Review of literature

The mean ± SD of previously reported errors of localization in studies of frameless stereotactic neuronavigation (not including the present study) was  $2.07 \pm 1.16$  mm [Table 2].

## DISCUSSION

Our preliminary data demonstrates that the image-based preoperative vascular and neural element segmentation, especially with 3D reconstruction, is highly informative for both preoperative planning and intraoperative navigation, particularly with complex tumors that invade and distort neurovascular and osseous structures. Image-guidance based neuronavigation will enhance the efficacy and safety of skull base surgery and can aid in directing the surgeon's attention to the nearby neurovascular structures. Neuronavigation is increasingly utilized in neurosurgery.<sup>[9,10,33,42]</sup> Its efficacy in the treatment of skull base tumors has already been shown.<sup>[7]</sup> With its high application fidelity, the system presented in this study provides genuinely useful feedback to the surgeon for case-specific anatomic orientation, planning, and simulation of the surgical approach, intraoperative guidance, identification and avoidance of vital neurovascular elements, and assessment of the extent of possible resection. It provides information about the interface between the tumor and normal tissue, the tumor's proximity to critical structures, and the possible location of the residual tumor.

Vessels and cranial nerves that are invaded, encased, or displaced by tumor may nevertheless be visualized on MRIs and displayed. Therefore, complex skull base tumors, in particular, benefit greatly from image-based preoperative vascular and neural element segmentation with 3D reconstruction. A number of important aspects of skull base surgery are discussed in the following paragraphs [Figures 1-3].

Neuronavigation offers real time visualization of any region of interest, including tumors and anatomic landmarks. Such image guidance data are easily marked, stored, and reconstructed in a 3D mode or any plane. Accordingly, the surgeon can preoperatively define the landmarks. Preoperatively creating and planning the surgical vectors is critically important, helps minimize cortical trauma, and provides the ability to determine the required extent of the surgical exposure. Additionally, image-guided preoperative planning indicates the appropriateness of a particular skull base approach.

Although the significance of brain shift on preoperatively acquired image guidance and the subsequent need for intraoperative image updating is a controversial and unresolved issue, it has been known for some time that skull base lesions have a remarkably small extent of intraoperative shift due to their anchoring to the bony structures of the skull base. As the skull base tumors are firmly attached to the dura and bone, and the cranial

**Table 2: Errors of localization in studies of frameless stereotactic neuronavigation reported in the literature**

Reference	Year	Work group	Navigation system	Coregistration technique	Errors of localization $\pm$ SD (mm)
Brinker <i>et al.</i> <sup>[3]</sup>	1998	Nordstadt Hospital, Hannover, Germany	Zeiss MKM	Paired point matching (bone screws)	0.7 $\pm$ 0.2
Dorward <i>et al.</i> <sup>[6]</sup>	1999	Neurosurgery, Royal Free Hospital, London, UK	EasyGuide Neuro frameless stereotactic navigation system (Philips)	Paired point matching (fiducial)	1.3 $\pm$ 0.6
Germano <i>et al.</i> <sup>[8]</sup>	1999	Neurosurgery, Mount Sinai Hospital, New York, NY	OD System	Paired point matching (fiducials)	1.7 $\pm$ 0.2
Golfinos <i>et al.</i> <sup>[9]</sup>	1995	Neurosurgery, St. Joseph's Hospital, Phoenix, AZ	FARO Surgicom	Paired point matching (fiducials)	2.8
Gumprecht <i>et al.</i> <sup>[10]</sup>	1999	Neurosurgery, München-Bogenhausen, Germany	BrainLab VectorVision	Paired point matching (fiducials)	4 $\pm$ 1.4
Hassfeld <i>et al.</i> <sup>[12]</sup>	1997	Maxillofacial and Craniofacial Surgery, University of Heidelberg, Germany	SPOCS (Aesculap)	Paired point matching (bone screws)	2
Helm and Eckel <sup>[13]</sup>	1998	Neuroradiology, Johns Hopkins Hospital, Baltimore, MD	FARO Surgicom (phantom study)	Paired point matching (fiducials)	2.1
Laborde <i>et al.</i> <sup>[21]</sup>	1992	Neurosurgery, Aachen, Germany	Computer-assisted localizer	Paired point matching (fiducials)	3
Marmulla <i>et al.</i> <sup>[25]</sup>	2004	Cranio-Maxillofacial Surgery, Heidelberg, Germany	SSN+ + (Carl Zeiss)	Surface matching (laser)	1.2 $\pm$ 0.3
Pfisterer <i>et al.</i> <sup>[27]</sup>	2008	Neurosurgery, St. Joseph's Hospital, Phoenix, AZ	StealthStation (Medtronic)	Surface matching (pointer)	3.3 $\pm$ 1.7
Pillai <i>et al.</i> <sup>[28]</sup>	2008	Neurosurgery, The Ohio State University Medical Center, Columbus, OH	Stryker Navigation System	Paired point matching (bone screws)	0.91 $\pm$ 0.28
Raabe <i>et al.</i> <sup>[29]</sup>	2002	Neurosurgery, Frankfurt am Main, Germany	BrainLab VectorVision2	Surface matching (laser)	1.8 $\pm$ 0.8
Ryan <i>et al.</i> <sup>[30]</sup>	1996	Neurosurgery, University of Chicago, Chicago, IL	Flashpoint 3D digitizer and Sparcstation2 (Sun)	Surface matching (misc.)	4.8 $\pm$ 3.5
Shamir <i>et al.</i> <sup>[31]</sup>	2009	Neurosurgery, Hebrew University, Jerusalem, Israel	FaceScan II (Brueckmann)	Surface matching (misc.)	0.9
Sipos <i>et al.</i> <sup>[33]</sup>	1996	Neurosurgery, Johns Hopkins Hospital, Baltimore, MD	FARO Surgicom	Paired point matching (fiducials)	2.3
Stidd <i>et al.</i> <sup>[36]</sup>	2014	Neurosurgery, Rush University Medical Center, Chicago, IL	StealthStation S7 (Medtronic)	Surface-based facial registration (laser)	0.71 $\pm$ 0.25
Stieglitz <i>et al.</i> <sup>[37]</sup>	2013	Neurosurgery, Bern University Hospital, Bern, Switzerland	BrainLab VectorVision2 and StealthStation (Medtronic)	Multiple	2.9 $\pm$ 3.3
Thompson <i>et al.</i> <sup>[39]</sup>	2011	Neurosurgery, Oregon Health and Science University, Portland, OR	StealthStation (Medtronic)	Paired point matching (bone screws)	1.3 $\pm$ 0.5
Villalobos and Germano <sup>[40]</sup>	1999	Neurosurgery, Mount Sinai Hospital, New York, NY	OD System	Paired point matching (fiducials)	1.6 $\pm$ 0.1
Watanabe <i>et al.</i> <sup>[42]</sup>	1991	Neurosurgery, Tokyo, Japan	Neuronavigator	Paired point matching (fiducials)	2.5
Woerdeman <i>et al.</i> <sup>[44]</sup>	2007	Neurosurgery, Rudolf-Magnus-Institute of Neuroscience, Utrecht, the Netherlands	StealthStation TREON Plus (Medtronic)	Paired point matching (fiducials)	1.9 $\pm$ 0.8
Wolfsberger <i>et al.</i> <sup>[45]</sup>	2002	University of Vienna Medical School, Vienna, Austria	EasyGuide Neuro frameless stereotactic navigation system (Philips)	Paired point matching (fiducials)	2.9 $\pm$ 1.0
Zinreich <i>et al.</i> <sup>[47]</sup>	1993	Neuroradiology, Johns Hopkins Hospital, Baltimore, MD	FARO Surgicom (phantom study)	Paired point matching (fiducials)	1-2 mm; $P > 95\%$
Present study	2014	Present Institution	BrainLab iPlan Net (8/10 patients) and Stryker (2/10 patients)	Paired point matching (fiducials)	Mean+SD: 0.45 $\pm$ 0.21

SD: Standard deviation, mm: Millimeters, 3D: Three-dimensional

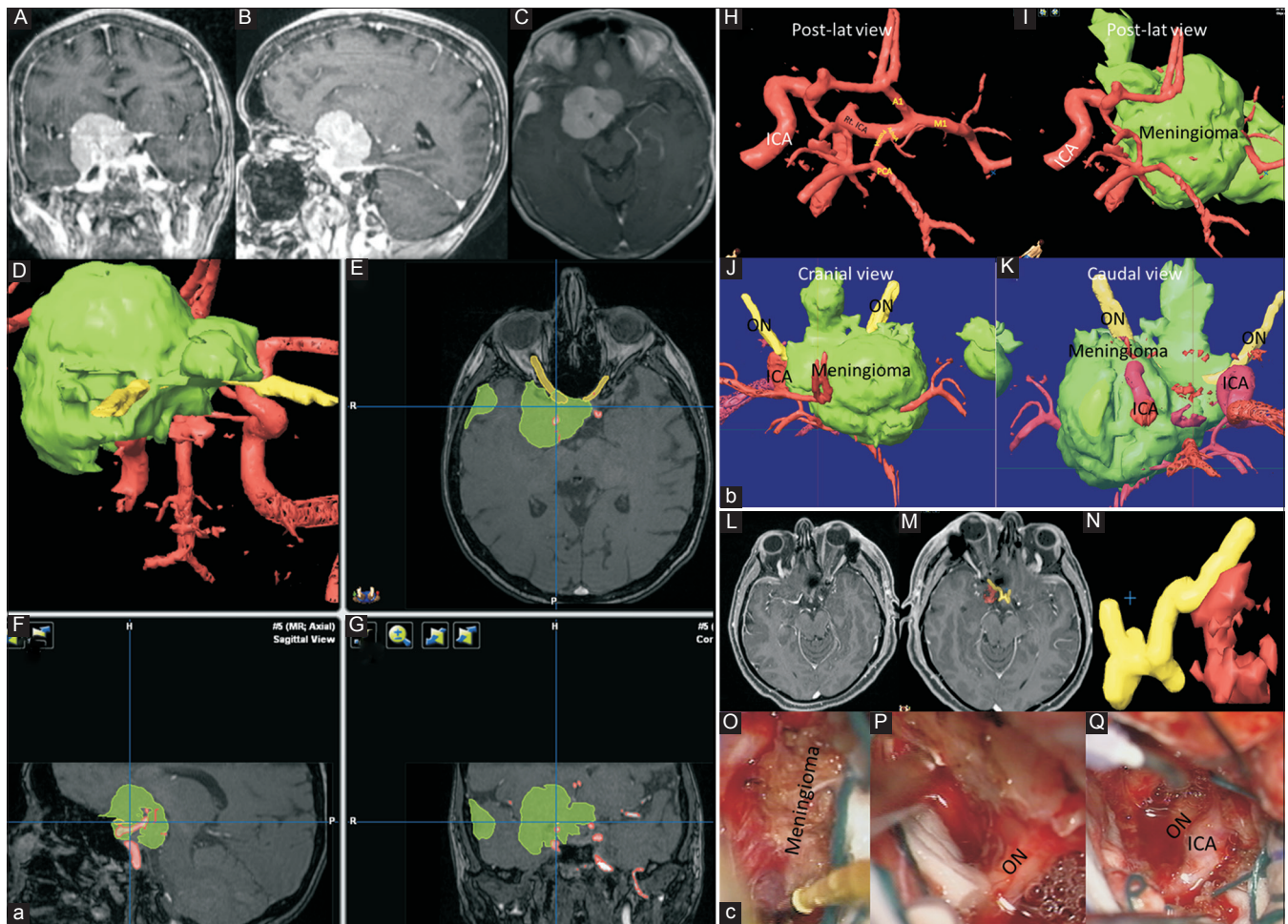


**Figure 2:** (a) A 55-year-old female presented with the progressive right visual loss. Panels A, B, and C show preoperative brain magnetic resonance imaging with gadolinium enhancement in coronal, sagittal, and axial views, respectively. Panels D, E, F, and G show preoperative segmentation of the tumor (green), optic and third nerves (yellow) and internal carotid artery and its branches using iPlan Net of BrainLAB system. (b) Panels H, I, J, and K show the preoperative segmentation of internal carotid artery and its branches (red), optic nerves (yellow), and tumor (green) of above-mentioned patient in detail. This patient underwent craniotomy and complete resection. (c) Panel L shows postoperative brain magnetic resonance imaging with gadolinium enhancement, Panels M (cranial view) and N (caudal view) show postoperative segmentation of optic nerve (yellow) and internal carotid artery (red), Panel O shows the meningioma encasing the right optic nerve and internal carotid artery and Panel P after decompression of the optic nerve and Panel Q, after decompressing of both optic nerve and internal carotid artery

nerves and the major blood vessels have relatively stable and protected position and course in this anatomic region, therefore, shift will not be a problem in neuronavigation in these cases. This feature indicates that image guidance offers a high degree of reliability for neuronavigation in the treatment of skull base lesions.<sup>[7]</sup> Brain shift due to cerebrospinal fluid loss did not significantly affect intraoperative image guidance in this study, which mirrors the results reported in the literature.<sup>[7]</sup> As such, skull base surgery seems to be especially well suited for image-guidance technology. Because the bony and neurovascular structures move far less during surgical manipulation than in any other type of neurosurgery, the tremendous advantage of neuronavigation becomes fully realized during the treatment of skull base pathologies. Therefore, the more expensive and time-intensive

intraoperative MRI-based image updating techniques may play only a minor role for skull base surgeries.<sup>[35]</sup>

Preliminary evaluations of the use of preoperative 3D image segmentation and patient registration have been reported for the surgery of aneurysms, meningioma, gliomas, pituitary tumors, cerebral cavernoma, and arteriovenous malformations.<sup>[4,14-18,23,34]</sup> While several groups have evaluated the use of preoperative 3D image segmentation and patient registration for skull base tumor resection surgeries,<sup>[11,26]</sup> these studies did not investigate spatial accuracy of preoperative image segmentation with intraoperative data. Additionally, they did not register the imaging data into the intraoperative neuronavigation system.<sup>[26]</sup> To our knowledge, this study represents the first to describe the use of vascular and neural element

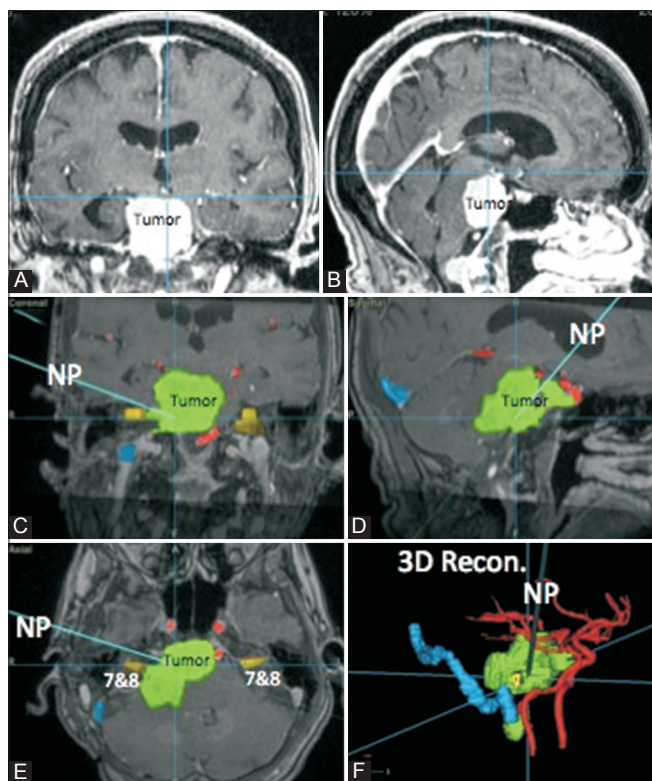


**Figure 3: Intraoperative neuronavigation for a 70-year-old female [Case 9 of Table 1] with a clival meningioma (Panels A and B) using preoperative segmentation of the tumor, internal carotid and vertebral arteries, and 7 and 8 nerves on Stryker neuronavigation system (Panels C-F). Navigation probe shows how close we are to the 7- and 8-nerve complex**

segmentation with 3D reconstruction during skull base surgery while also assessing the accuracy of preoperative image segmentation with intraoperative data.

In our study, very good correspondence between image-based segmentation and the microscopic view was found at the surface of the tumor and tumor-normal brain interfaces in all cases [Figure 2]. Also, preoperative segmentation of the major arteries, veins, and venous sinuses matched with the intraoperative microscopic findings. This information reassured the surgeon and prevented vascular injury during different stages of tumor resection. Image-based segmentation also helped in preventing major intraoperative arterial or venous bleeding [Figures 1 and 2]. Preoperative segmentation of the related cranial nerves was technically possible in only 80% of cases. However, image-guidance helped the surgeon to localize the involved cranial nerves in all cases [Figures 1 and 2]. Thus, image-based segmentation has a large utility for skull base tumor surgery.

In our experience, the prompt identification, and thus circumvention, of invaded, encased, or displaced vital neurovascular structures during tumor dissection is the most imperative advantage that is, offered by neuronavigation, especially when tumor encasing important

neurovascular structure of the brain [Figures 2 and 3]. Our data reflects the results reported by other studies examining image-guided skull base tumor resections. These studies have found gross total resection rates between 80% and 94.25% of cases, new permanent cranial nerve deficits from 0% to 23% of cases, and postoperative mortality between 0% and 4.6%.<sup>[19,20,38,43]</sup>

The image-guided skull base surgery data demonstrates an improvement over comparable nonimage guided skull base surgery data. Several nonimage guided skull base surgery studies report gross total resection rates from 61% to 79%, new permanent cranial nerve deficits from 25% to 76%, and mortality rates from 0% to 11%,<sup>[2,5,22,46]</sup> indicating that the widespread adoption of image-guidance for skull base surgery may be clinically indicated.

Therefore, we believe that the use of image-based preoperative vascular and neural element segmentation, especially with 3D reconstruction and intraoperative application of these data for navigation, as presented in our series might additionally help minimize the morbidity rate in patients suffering from extensive skull base lesions. Especially, in situations of complex anatomy or when the abnormality involves critical structures, navigational tools are likely to be beneficial, reducing operative time and increasing the safety of surgery. Image guidance can be very useful for enhancing the confidence of localizing vascular structures, tumor extension, and the osseous structures, particularly in less experienced neurosurgeons [Figures 1-3].

Neuronavigation only provides surgical utility if the image guidance system data accurately corresponds to the perioperative patient anatomy. A previous retrospective review of the literature found that mean neuronavigation accuracies have ranged from 0.7 to 5 mm.<sup>[37]</sup> The studies reporting the least errors of localization (0.7–2 mm) used the paired point matching by bone screws method for coregistration.<sup>[3,12,28,39]</sup> While accurate, bone screw placement has the disadvantage of being an invasive procedure.

Recently, one group has reported an accuracy similar to that obtained by paired point matching by bone screws, using the technique of preoperatively acquired 3D digital subtraction angiography (DSA) registered by the facial surface anatomy contained within the data set.<sup>[36]</sup> The investigators validated their novel neuronavigation technique in a cadaver model and reported an accuracy of  $0.71 \pm 0.25$  mm (mean  $\pm$  standard error).<sup>[36]</sup> This accuracy may be overestimated, as the brain tissue and cerebrovasculature of their cadaver model were relatively anchored in place due to formalin fixation and injection of the vasculature with latex. Thus, the accuracy-degrading complication of perioperative brain shift was largely eliminated. While DSA remains the

gold standard for imaging of cerebrovascular pathology due to its superior detection sensitivity and spatial resolution over MR angiography and CT angiography,<sup>[1]</sup> the imaging modality is not without its limitations and risks. Although DSA offers a high spatial resolution of the cerebral vasculature, it provides only limited anatomical information about extravascular structures, knowledge of which may minimize surgical morbidity and mortality. According to our review of the literature, the mean  $\pm$  SD of previously reported errors of localization literature was  $2.07 \pm 1.16$  mm [Table 2].

Our group achieved a measurement accuracy of  $0.45 \pm 0.21$  mm (mean  $\pm$  SD), which is improved over previously reported accuracies ranging from 0.7 to 5 mm.<sup>[3,6,8-10,12,13,21,25,27-31,33,36,37,39-41,44,45,47]</sup> Additionally, we utilized preoperative 3T MRI and dynamic CT angiography for image acquisition, which are far less invasive procedures than DSA. We also used paired point matching by fiducials, which are far less invasive to place than bone screws. Finally, our neuronavigation system was validated in living patients, so our reported accuracy includes effects of surgically induced shifts.

For experienced surgeons, bony and neurovascular landmarks represent the best and most consistent navigational tools for avoiding neural and vascular compromise. However, using the currently described image-based vascular and cranial nerve segmentation technique confers several additional benefits, particularly for less experienced surgeons. First, the surgeon commits spending time for preoperative segmentation of the neurovascular elements in the course of access to the target tumor, which will aid in the understanding of these anatomical landmarks in advance. Second, these bony and neurovascular anatomical landmarks are not fixed in all cases. Therefore, preoperative segmentation will detect anatomical variations and warn the attending surgeon to start or continue the approach from a direction which has the least chance of causing vascular or cranial nerve injuries. Finally, the availability of a 3D segmented real time navigational tool is reassuring for less experienced neurosurgeons.

## CONCLUSION

Image-based preoperative vascular and neural element segmentation, especially with 3D reconstruction, is highly informative for both preoperative planning and intraoperative navigation, particularly with complex skull base tumors that invade and distort neurovascular and osseous structures. Image-guidance based neuronavigation enhances the efficacy and safety of skull base surgery, in part by increasing the surgeon's vigilance, and helps to avoid vascular and neural injury during skull base surgeries. Additionally, the accuracy found in this study is superior to previously reported neuronavigation

measurements, mostly because of the minimal brain shift encountered in skull base tumor surgeries. This novel preliminary study is encouraging for future prospective intraoperative validation with larger numbers of patients.

## Financial support and sponsorship

Nil.

## Conflicts of interest

There are no conflict of interest.

## REFERENCES

1. Anxionnat R, Bracard S, Ducrocq X, Troussat Y, Launay L, Kerrien E, et al. Intracranial aneurysms: Clinical value of 3D digital subtraction angiography in the therapeutic decision and endovascular treatment. *Radiology* 2001;218:799-808.
2. Bricolo AP, Turazzi S, Talacchi A, Cristofori L. Microsurgical removal of petroclival meningiomas: A report of 33 patients. *Neurosurgery* 1992;31:813-28.
3. Brinker T, Arango G, Kaminsky J, Samii A, Thorns U, Vorkapic P, et al. An experimental approach to image guided skull base surgery employing a microscope-based neuronavigation system. *Acta Neurochir (Wien)* 1998;140:883-9.
4. Cabrilo I, Bijlenga P, Schaller K. Augmented reality in the surgery of cerebral aneurysms: A technical report. *Neurosurgery* 2014;10 Suppl 2:252-60.
5. Di Maio S, Rostomily R, Sekhar LN. Current surgical outcomes for cranial base chordomas: Cohort study of 95 patients. *Neurosurgery* 2012;70:1355-60.
6. Dorward NL, Alberti O, Palmer JD, Kitchen ND, Thomas DG. Accuracy of true frameless stereotaxy: *In vivo* measurement and laboratory phantom studies. Technical note. *J Neurosurg* 1999;90:160-8.
7. Dorward NL, Alberti O, Velani B, Gerritsen FA, Harkness WF, Kitchen ND, et al. Postimaging brain distortion: Magnitude, correlates, and impact on neuronavigation. *J Neurosurg* 1998;88:656-62.
8. Germano IM, Villalobos H, Silvers A, Post KD. Clinical use of the optical digitizer for intracranial neuronavigation. *Neurosurgery* 1999;45:261-9.
9. Golfinos JG, Fitzpatrick BC, Smith LR, Spetzler RF. Clinical use of a frameless stereotactic arm: Results of 325 cases. *J Neurosurg* 1995;83:197-205.
10. Gumprecht HK, Widenka DC, Lumenta CB. BrainLab VectorVision Neuronavigation System: Technology and clinical experiences in 131 cases. *Neurosurgery* 1999;44:97-104.
11. Haerle SK, Daly MJ, Chan HH, Vescan A, Kucharczyk W, Irish JC. Virtual surgical planning in endoscopic skull base surgery. *Laryngoscope* 2013;123:2935-9.
12. Hassfeld S, Muehling J, Wirtz CR, Knauth M, Lutze T, Schulz HJ. Intraoperative guidance in maxillofacial and craniofacial surgery. *Proc Inst Mech Eng H* 1997;211:277-83.
13. Helm PA, Eckel TS. Accuracy of registration methods in frameless stereotaxis. *Comput Aided Surg* 1998;3:51-6.
14. Inoue D, Cho B, Mori M, Kikkawa Y, Amano T, Nakamizo A, et al. Preliminary study on the clinical application of augmented reality neuronavigation. *J Neurol Surg A Cent Eur Neurosurg* 2013;74:71-6.
15. Kawamata T, Iseki H, Shibasaki T, Hori T. Endoscopic augmented reality navigation system for endonasal transsphenoidal surgery to treat pituitary tumors: Technical note. *Neurosurgery* 2002;50:1393-7.
16. Kersten-Oertel M, Chen SS, Drouin S, Sinclair DS, Collins DL. Augmented reality visualization for guidance in neurovascular surgery. *Stud Health Technol Inform* 2012;173:225-9.
17. King AP, Edwards PJ, Maurer CR Jr, de Cunha DA, Hawkes DJ, Hill DL, et al. A system for microscope-assisted guided interventions. *Stereotact Funct Neurosurg* 1999;72:107-11.
18. Kockro RA, Tsai YT, Ng I, Hwang P, Zhu C, Agusanto K, et al. Dex-ray: Augmented reality neurosurgical navigation with a handheld video probe. *Neurosurgery* 2009;65:795-807.
19. Kurtsoy A, Menku A, Tucer B, Oktom IS, Akdemir H. Neuronavigation in skull base tumors. *Minim Invasive Neurosurg* 2005;48:7-12.



20. Kurtsoy A, Menku A, Tucer B, Suat Oktem I, Akdemir H, Kemal Koc R. Transbasal approaches: Surgical details, pitfalls and avoidances. *Neurosurg Rev* 2004;27:267-73.
21. Laborde G, Gilsbach J, Harders A, Klimek L, Moesges R, Krybus W. Computer assisted localizer for planning of surgery and intra-operative orientation. *Acta Neurochir (Wien)* 1992;119:166-70.
22. Lang DA, Honeybul S, Neil-Dwyer G, Evans BT, Weller RO, Gill J. The extended transbasal approach: Clinical applications and complications. *Acta Neurochir (Wien)* 1999;141:579-85.
23. Low D, Lee CK, Dip LL, Ng WH, Ang BT, Ng I. Augmented reality neurosurgical planning and navigation for surgical excision of parasagittal, falx and convexity meningiomas. *Br J Neurosurg* 2010;24:69-74.
24. Maciunas RJ. Intraoperative cranial navigation. *Clin Neurosurg* 1996;43:353-81.
25. Marmulla R, Mühling J, Wirtz CR, Hassfeld S. High-resolution laser surface scanning for patient registration in cranial computer-assisted surgery. *Minim Invasive Neurosurg* 2004;47:72-8.
26. Oishi M, Fukuda M, Yajima N, Yoshida K, Takahashi M, Hiraishi T, et al. Interactive presurgical simulation applying advanced 3D imaging and modeling techniques for skull base and deep tumors. *J Neurosurg* 2013;119:94-105.
27. Pfisterer WK, Papadopoulos S, Drumm DA, Smith K, Preul MC. Fiducial versus nonfiducial neuronavigation registration assessment and considerations of accuracy. *Neurosurgery* 2008;62 3 Suppl 1:201-7.
28. Pillai P, Sammet S, Ammirati M. Application accuracy of computed tomography-based, image-guided navigation of temporal bone. *Neurosurgery* 2008;63 4 Suppl 2:326-32.
29. Raabe A, Krishnan R, Wolff R, Hermann E, Zimmermann M, Seifert V. Laser surface scanning for patient registration in intracranial image-guided surgery. *Neurosurgery* 2002;50:797-801.
30. Ryan MJ, Erickson RK, Levin DN, Pelizzari CA, Macdonald RL, Dohrmann GJ. Frameless stereotaxy with real-time tracking of patient head movement and retrospective patient-image registration. *J Neurosurg* 1996;85:287-92.
31. Shamir RR, Freiman M, Joskowicz L, Spektor S, Shoshan Y. Surface-based facial scan registration in neuronavigation procedures: A clinical study. *J Neurosurg* 2009;111:1201-6.
32. Simpson D. The recurrence of intracranial meningiomas after surgical treatment. *J Neurol Neurosurg Psychiatry* 1957;20:22-39.
33. Sipos EP, Tebo SA, Zinreich SJ, Long DM, Brem H. *In vivo* accuracy testing and clinical experience with the ISG Viewing Wand. *Neurosurgery* 1996;39:194-202.
34. Stadie AT, Reisch R, Kockro RA, Fischer G, Schwandt E, Boor S, et al. Minimally invasive cerebral cavernoma surgery using keyhole approaches-solutions for technique-related limitations. *Minim Invasive Neurosurg* 2009;52:9-16.
35. Steinmeier R, Fahlbusch R, Ganslandt O, Nimsky C, Buchfelder M, Kaus M, et al. Intraoperative magnetic resonance imaging with the magnetom open scanner: Concepts, neurosurgical indications, and procedures: A preliminary report. *Neurosurgery* 1998;43:739-47.
36. Stidd DA, Wewel J, Ghods AJ, Munich S, Serici A, Keigher KM, et al. Frameless neuronavigation based only on 3D digital subtraction angiography using surface-based facial registration. *J Neurosurg* 2014;121:745-50.
37. Stieglitz LH, Fichtner J, Andres R, Schucht P, Krähenbühl AK, Raabe A, et al. The silent loss of neuronavigation accuracy: A systematic retrospective analysis of factors influencing the mismatch of frameless stereotactic systems in cranial neurosurgery. *Neurosurgery* 2013;72:796-807.
38. Sure U, Alberti O, Petermeyer M, Becker R, Bertalanffy H. Advanced image-guided skull base surgery. *Surg Neurol* 2000;53:563-72.
39. Thompson EM, Anderson GJ, Roberts CM, Hunt MA, Selden NR. Skull-fixated fiducial markers improve accuracy in staged frameless stereotactic epilepsy surgery in children. *J Neurosurg Pediatr* 2011;7:116-9.
40. Villalobos H, Germano IM. Clinical evaluation of multimodality registration in frameless stereotaxy. *Comput Aided Surg* 1999;4:45-9.
41. Watanabe E, Mayanagi Y, Kosugi Y, Manaka S, Takakura K. Open surgery assisted by the neuronavigator, a stereotactic, articulated, sensitive arm. *Neurosurgery* 1991;28:792-9.
42. Watanabe E, Watanabe T, Manaka S, Mayanagi Y, Takakura K. Three-dimensional digitizer (neuronavigator): New equipment for computed tomography-guided stereotaxic surgery. *Surg Neurol* 1987;27:543-7.
43. Wiltfang J, Rupperecht S, Ganslandt O, Nimsky C, Keßler P, Schultze-Mosgau S, et al. Intraoperative image-guided surgery of the lateral and anterior skull base in patients with tumors or trauma. *Skull Base* 2003;13:21-29.
44. Woerdeman PA, Willems PW, Noordmans HJ, Tulleken CA, van der Sprenkel JW. Application accuracy in frameless image-guided neurosurgery: A comparison study of three patient-to-image registration methods. *J Neurosurg* 2007;106:1012-6.
45. Wolfsberger S, Rössler K, Regatschnig R, Ungersböck K. Anatomical landmarks for image registration in frameless stereotactic neuronavigation. *Neurosurg Rev* 2002;25:68-72.
46. Xu F, Karampelas I, Megerian CA, Selman WR, Bambakidis NC. Petroclival meningiomas: An update on surgical approaches, decision making, and treatment results. *Neurosurg Focus* 2013;35:E11.
47. Zinreich SJ, Tebo SA, Long DM, Brem H, Mattox DE, Loury ME, et al. Frameless stereotaxic integration of CT imaging data: Accuracy and initial applications. *Radiology* 1993;188:735-42.